



Mathematical modeling and simulation of hydrogen-fueled solid oxide fuel cell system for micro-grid applications - Effect of failure and degradation on transient performance

Konrad W. Eichhorn Colombo ^{a,*}, Vladislav V. Kharton ^b, Filippo Berto ^c,
Nicola Paltrinieri ^c

^a Department of Chemical Engineering, Norwegian University of Science and Technology (NTNU), Trondheim, Norway

^b Institute of Solid State Physics, Moscow District, Chernogolovka, Russian Federation

^c Department of Mechanical and Industrial Engineering, NTNU, Trondheim, Norway

ARTICLE INFO

Article history:

Received 7 November 2019

Received in revised form

27 April 2020

Accepted 29 April 2020

Available online 6 May 2020

Keywords:

Solid oxide fuel cell (SOFC)

System analysis

Mathematical model

Micro-grid

Degradation

Failure

Transient simulation

Degrees of freedom

Controlled and manipulated variables

ABSTRACT

We use a detailed solid oxide fuel cell (SOFC) model for micro-grid applications to analyze the effect of failure and degradation on system performance. Design and operational constraints on a component- and system level are presented. A degrees of freedom analysis identifies controlled and manipulated system variables which are important for control. Experimental data are included to model complex degradation phenomena of the SOFC unit. Rather than using a constant value, a spatially distributed degradation rate as function of temperature and current density is used that allows to study trajectory-based performance deterioration. The SOFC unit is assumed to consist of multiple stacks. The failure scenario studied is the loss of one individual SOFC stack, e.g. due to breakage of sealing or a series of fuel cells. Simulations reveal that degradation leads to significant drifts from the design operating point. Moreover, failure of individual stacks may bring the still operating power generation unit into a regime where further failures and accelerated degradation is more likely. It is shown that system design, dimensioning, operation and control are strongly linked. Apart from specific quantitative results perhaps the main practical contribution are the collected constraints and the degrees of freedom analysis.

© 2020 The Authors. Published by Elsevier Ltd. This is an open access article under the CC BY license (<http://creativecommons.org/licenses/by/4.0/>).

1. Introduction

Fuel cell systems continue to receive much attention due to their potential as a crucial building block for green energy solutions. Relatively high efficiencies of more than 60% can be obtained [1–3]. On this thread, the most promising fuel cell types for application in micro-combined heat and power (CHP) systems are proton exchange membrane fuel cell (PEMFC) and solid oxide fuel cell (SOFC) technologies. Ref. [4] provides an overview of commercialized (and near-term) FC-based micro-CHP systems, and various studies discussed CHP applications with SOFCs [5,6], for example using a two-stage thermoelectric generator [7]. Refs. [8,9] are few of several studies in which SOFC-based hybrid cycles with gas turbines are discussed. However, a higher degree of system integration, for

example due to waste heat recovery, usually also leads to additional operational constraints, an increased overall system complexity as well as the need for further process equipment. We therefore use one of the most basic SOFC-based configurations to emphasize the main aspects in this work, namely the effect of failure and degradation on transient system performance.

Due to high operating temperatures, SOFCs can employ non-precious metal and earth-abundant oxide electro-catalysts. Furthermore, in SOFC systems gaseous and liquid hydrocarbons as well as solid fuels¹ can be utilized and converted into electricity. Operation of SOFCs in reverse mode offers, in principle, the opportunity to produce fuels at low power demand, which can afterwards be consumed again by the system [10–12]. However, such switching may be problematic from a lifetime point of view [13–15] and also lead to additional requirements in terms of functional

* Corresponding author.

E-mail address: konrad.eichhorn@ntnu.no (K.W. Eichhorn Colombo).

¹ Including biomass and coal.

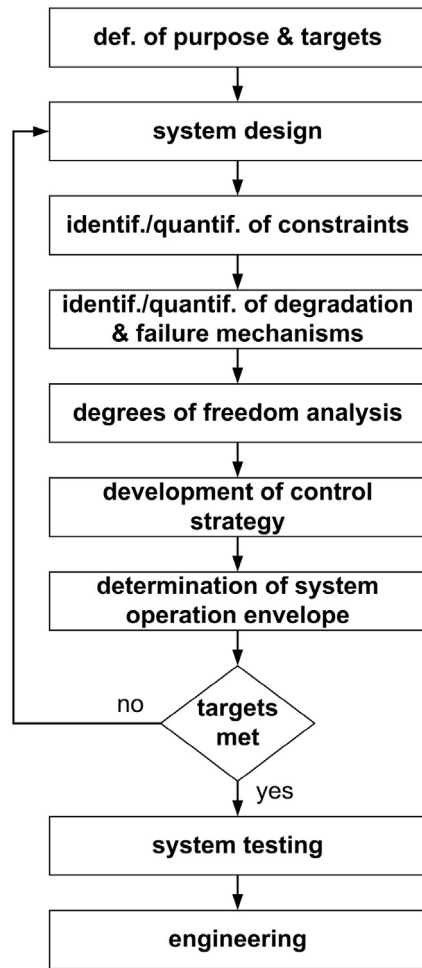


Fig. 1. Overall methodology for system design comprising identification of constraints and degree of freedom analysis.

components and drifts due to activation and degradation phenomena. And within reliability the trend seems to go towards increasingly complex methods and mathematical models, for example to define mixture probability models of systems but frequently without taking into account the structure and dynamics of the actual physics. This paper is intended to exemplify the strong interdependence of the three aforementioned disciplines. The applied methods can be used for other systems than SOFC-based processes, for example to improve system performance and lifetime. Rather than focusing on maximizing only few properties, (e.g., kinetics and mass transport), a stronger system perspective is needed to find materials and designs for flexibility in steady-state and transient operation. Advantages of the detailed model-based approach for degradation and failure analyses used in this work include that factor and shape for acceleration can easily be incorporated. It is worth mentioning that the model-based approach should not replace physical testing but is complementary to it, for instance to identify critical tests and to avoid unnecessary redesigns which often are time and cost-intensive.

2. Process system model

Only basic explanations about the physics and chemistry of processes in the SOFC system are provided in this section. For further explanations Refs. [25–30] can be consulted. The process flow diagram with some key assumptions and results for the design

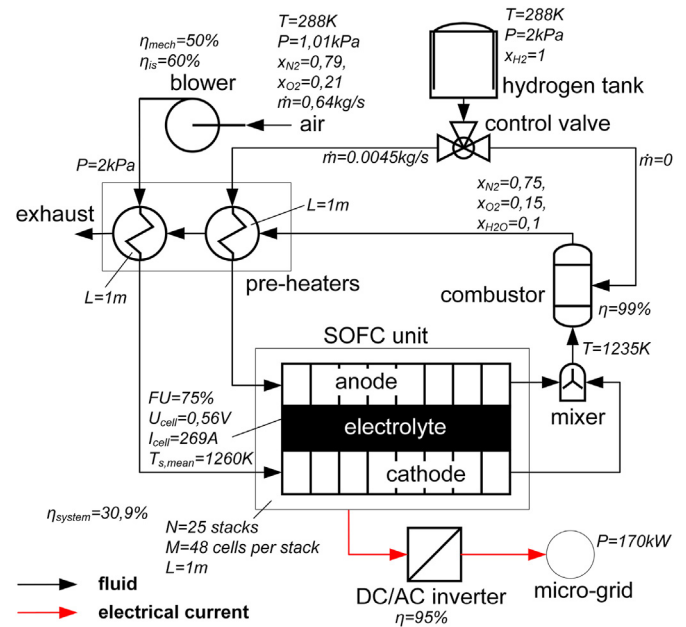


Fig. 2. Process flow diagram of the hydrogen-fueled solid oxide fuel system with some key assumptions and design simulation results.

case is shown in Fig. 2² Air is fed to the system by means of a blower. Pure hydrogen is assumed as fuel. Consequently, steam and oxygen-depleted air are the only emitted gases. Fuels containing carbon or impurities would favor further potential degradation mechanisms [33–35]. No additional fuel is fed to the combustor, but this may be required for start-up and shutdown. Direct current (DC) is produced in the SOFC unit and converted to alternating current (AC) in the DC/AC inverter, before being fed to the micro-grid. Unconverted effluent hydrogen is burned in the combustor. The hydrogen that can be fed to the combustor provides an additional degree of freedom. The heat in the exhaust gas is utilized to preheat the fuel and air. The blower compresses the air to pressures to minimize the pressure difference between fuel and air to minimize mechanical loads.

2.1. Solid oxide fuel cell

A simplified fuel cell scheme comprises five components, i.e. two gas channels and three ceramic or composite layers. Its operation requires also two metallic current collectors (interconnects) and a sealant. The gas channels provide the fluid for reduction (cathode) and oxidation (anode), respectively. Between the two electrodes (anode and cathode) there is an oxygen-ion conducting solid electrolyte. Charge neutrality and movement of negative charges (electrons) is provided through an outer electrical circuit. Fig. 3 shows the principal mechanism in an individual cell.

In the electrochemical cell oxygen ions are transported from the cathode across the electrolyte membrane to the anode according to the following half-cell reactions on the cathode (oxygen reduction) and the anode (fuel oxidation), respectively [30]



² Combustor efficiency was taken from Ref. [31], blower and DC/AC inverter efficiencies from Ref. [32].

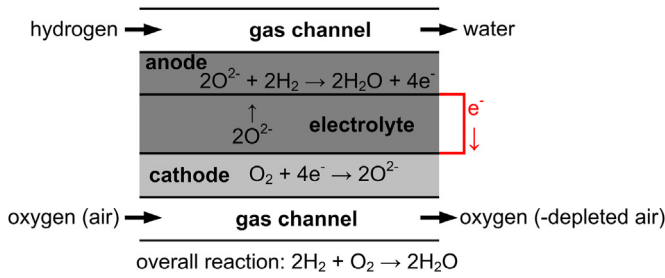
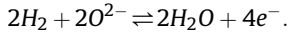
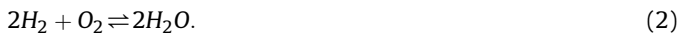


Fig. 3. Principle of a solid oxide fuel cell (SOFC) with hydrogen as fuel.



The resulting global equilibrium reaction is



Elevated temperatures in excess of 500°C are needed for the ceramic electrodes to become electrochemically active. The currently most common anode material for SOFCs is the ceramic-metal composite (cermet) of nickel and yttria-stabilized zirconia (Ni-YSZ), for cathode material it is strontium-doped LaMnO_3 (LSM), and for electrolyte materials it is YSZ and other zirconia-based phases with cubic or tetragonal structure. One of the SOFC layers is also used for mechanical support of the entire membrane-electrode assembly (MEA) and is hence the thickest part of the fuel cell. For long-term stability, a sufficient match in terms of thermo-mechanical and -chemical properties of the SOFC materials is critical [30,36].

In this work, a tubular design of the SOFC is assumed, shown in Fig. 4 with part of the repeating manifold of the stack and cell design [27,28,37–39]. $N = 25$ stacks with $M = 48$ cells each are assumed. Table 1 provides some advantages and drawbacks of the tubular and planar design, i.e. of the most common designs. Both have their individual strengths and weaknesses. Other designs include flat tubular-, bell-and-spigot- [40] and micro-tubular designs [41,42]. Further information about fuel cell designs is given in Ref. [37]. The SOFC unit in this work has N stacks and M cells. The

Table 1
Advantages and drawbacks of different SOFC geometries [30,41,42,44].

planar		tubular	
advantages	drawbacks	advantages	drawbacks
manufacturing cost	thermal (cycling) stability	thermal (cycling) stability	ohmic loss
power density	gas sealing	gas sealing	power density

principle component models from Ref. [43] were used and extended for this analyses. A parallel configuration was assumed.

There is no lack of SOFC models in the literature with a varying level of detail, ranging from steady-state lumped to spatially distributed dynamic models [45–48]. For our purposes a spatially distributed dynamic model in the axial direction provides a balance between level of detail and computational cost. Critical physical phenomena on different time-scales can be captured by this model. The electrochemical reactions have time constants within less than a second [18] and thermal transients in the range of minutes. Mass transport phenomena at high temperatures occur on time scales between those of electrochemistry and heat transport. Transient time constants especially those for heat and mass transport strongly depend on operating conditions [49–51]. Degradation usually occurs over time periods of several hundred hours.

2.1.1. Energy conservation

Heat transfer between the gases and solids is spatially distributed in one dimension [9,43]

$$\frac{\partial T_g c_{p,g} \rho_g}{\partial t} + v_g \frac{\partial T_g c_{p,g} \rho_g}{\partial z} = \frac{2hc}{r} (T_s - T_g). \quad (3)$$

The spatially distributed energy balance in axial and radial direction for the solids is [9,43]

$$\rho_s c_{p,s} \frac{\partial T_s}{\partial t} = \lambda_s \nabla^2 T_s. \quad (4)$$

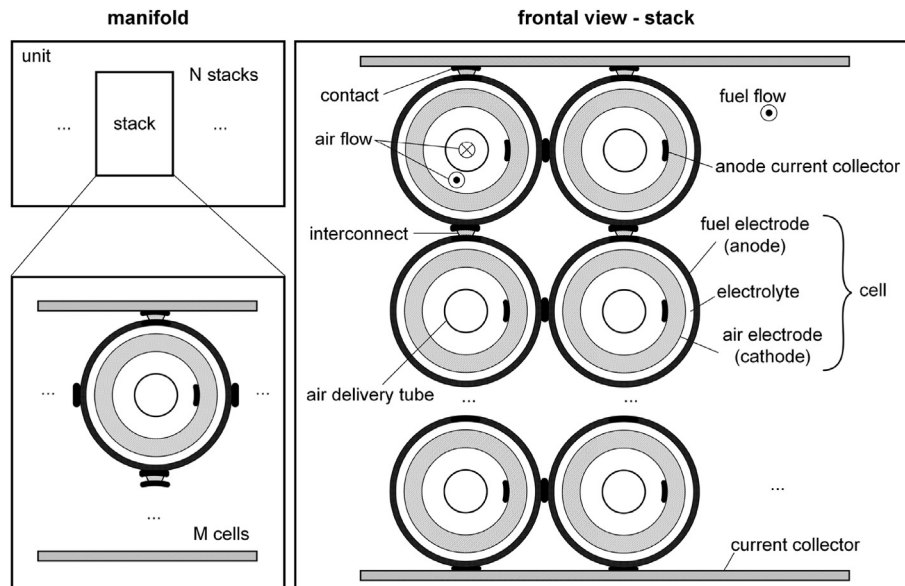


Fig. 4. SOFC unit with part of the repeating manifold of the tubular solid oxide fuel stacks and cells design.

2.1.2. Mass conservation

Mass conservation for the gases follows [9,43]

$$\frac{\partial C_i}{\partial t} + v_g \frac{\partial C_i}{\partial z} = \dot{r}_i. \quad (5)$$

2.1.3. Momentum conservation

Transients and spatial distributions in momentum were neglected. But pressure drops in both gas streams were considered using Reynolds number and friction factor correlations (laminar flow) according to [25,43]

$$\Delta P = c \frac{1}{2} \rho v^2. \quad (6)$$

2.1.4. Electrochemistry

The cell voltage is based on the overpotential approach where activation polarization, concentration polarization and ohmic losses reduce the theoretically possible open circuit voltage (OCV) [30]

$$V_{cell} = V_{OC} - \eta_{act}^{an} \left(1 + \dot{r}_{deg,act}^{an} \right) - \eta_{act}^{ca} \left(1 + \dot{r}_{deg,act}^{ca} \right) - \eta_{con}^{an} - \eta_{con}^{ca} - \eta_{ohm} \left(1 + \dot{r}_{deg,ohm} \right), \quad (7)$$

with \dot{r}_{deg} as the degradation rates for ohmic and activation overpotential losses. The OCV is given by the Nernst equation [30]

$$V_{OC} = E^\circ + \frac{RT}{zF} \ln \frac{a_{oxi}}{a_{red}}. \quad (8)$$

The activation polarization losses on anode and cathode are given implicitly by the Butler-Volmer equation [30]

$$i_i = i_i^\circ \left[\exp \left(\frac{n_i \beta_{ri} F \eta_{act,i}}{RT} \right) - \exp \left(- \frac{n_i \beta_{ri} F \eta_{act,i}}{RT} \right) \right], \quad (9)$$

which is frequently used for SOFC system analyses but also has some limitations [29,52].

The concentration polarization losses describe interactions between the bulk gas phase to electrode surfaces as well as between electrode surfaces and triple-phase boundary (TPB) reads [30]

$$\eta_{con,i} = \frac{RT}{n_i F} \ln \left(p_{i,g}, p_{i,TPB} \right). \quad (10)$$

The ohmic loss is [30]

$$\eta_{ohm} = iAR, \quad (11)$$

with an ohmic resistance comprising temperature-dependent layer resistivity of electrodes and electrolyte and a constant resistivity for the interconnects.

2.2. Combustor

The following global reaction is used to model combustion of hydrogen under oxygen-excess conditions



Equilibrium-based models with the same reaction have been modeled and tested. The results were the same, but numerical stability was challenging due to the value range of the reaction rate

constant [53]. The reactions are assumed to proceed in the forward direction only. For combustion systems in municipal areas emissions may be of concern.³ Heat and pressure losses are considered in the model.

2.3. Preheater

The preheaters are modeled as shell-and-tube heat exchangers, similar to the SOFC stack model but without the spatial distribution in radial direction. Effects of interaction between the individual parts of the manifold are neglected.

2.4. Fuel system and piping

The fuel system consists of tanks for hydrogen and control valves.⁴ Dynamics of the tanks are neglected. Piping models represent residence times in the system, these are assumed to be well insulated resulting in adiabatic conditions. A one-dimensional continuum equation is used and the pressure drop is based on an average of fluid density and velocity with a friction factor originally calculated implicitly with the Colebrook equation [55], which is simplified to arrive at an explicit function for improved numerical robustness during dynamic simulation.

2.5. Electrical power equipment

Electrical power equipment (here only DC/AC-inverter) is modeled with a fixed efficiency value. However, any performance deterioration due to off-design, degradation, or both, has a direct and hence strong effect on the overall system efficiency.

2.6. Solid oxide fuel cell system

The total current from the SOFC stack is

$$I_{cell} = \frac{A}{L} \int_0^L i(z) dz, \quad (13)$$

and the DC power from the SOFC stack is

$$P_{el} = V_{cell} I_{cell}. \quad (14)$$

Fuel utilization (FU) is calculated according to [30]

$$FU = \frac{I_{cell}}{2F \dot{n}_{fuel}}. \quad (15)$$

The electrical system efficiency is [6]

$$\eta_{el} = \frac{P_{el}}{\dot{m}_{fuel} LHV_{fuel}}. \quad (16)$$

And the mean solid temperature of the SOFC is

$$\bar{T}_s = \frac{1}{L} \int_0^L T(y, z) dy dz. \quad (17)$$

³ In addition to steam, NO_x may be formed (which can be represented by the Zeldovich mechanism [29]). It is however assumed here that combustion temperatures and residence times do not become excessive. Formation of NO_x is hence neglected.

⁴ For start-up and shutdown safety gas may be required [54].

3. Degrees of freedom, constraints, degradation and failure phenomena

Degradation and failure phenomena are strongly affected by constraints which arise due to design or operation on a system-, component- or part-level. Some constraints are hard and cannot be crossed, whilst others are soft and can be crossed but possibly at the expense of reduced performance, accelerated degradation and higher risk of failure. The relatively high degree of integration in the system leaves a set of few manipulated variables to manipulate setpoints to control certain variables.

3.1. Controlled and manipulated variables

The set of controlled and manipulated variable for the SOFC system is shown in Table 2. Other options for some of the variables are possible. A relative gain array analysis [56] can be applied to obtain pairing of controlled and manipulated variables which becomes important when developing and tuning controllers. The selection of pairs needs to take into account the measurability of the quantity and the response time. For example, electrical properties, such as stack current, usually respond faster than fluid properties, such as FU. In the presence of electrochemically reactive species at reaction sites (TPB), the SOFC can respond to load variations within the time scale of electrochemistry (within milliseconds [18]). FU must be regulated to avoid low operating temperatures. Quantities with a strong influence on system performance are cell voltage, fuel flow rate and stack inlet air temperature. An additional degree of freedom could be generated by splitting the air entering the system prior to the preheater, in other words a certain fraction can be bypassed to control the inlet temperature of air entering the SOFC unit. Our simulations showed however a relatively small benefit for operation. Furthermore, instead of using pure hydrogen as fuel, a hydrogen-steam mixture may be used, where the composition can be manipulated to control the electrochemical parameters in the SOFC unit to some extent. However, these two degrees of freedom are not analysed here, but are expected to be important for start-up and shutdown of the system. It is emphasized that control of combustor temperature may be difficult because of the potentially rapid changes and small thermal inertia, respectively, if the gas composition changes. This effect is stronger for small combustors [18].

3.2. Design and operation constraints

As mentioned above each system component and part may introduce constraints with a strong effect on the system level. Hence, the introduction of further process components need to be evaluated with a view to overall gain comprising criteria such as system flexibility and operability. A case in point is heat integration. From a thermodynamic efficiency point of view heat utilization should be maximized, but process complexity and hence flexibility may be compromised, in addition to higher cost due to additional

equipment. On the other hand, overall cost may also be reduced because of improved lifetime of the equipment.

The operational and material constraints for individual process units of the SOFC system are shown in Table 3, which define the region where the plant can be operated in a safe manner. Most of these constraints are critical and their violation can lead to irreversible and detrimental conditions, i.e. operation in regimes where constraints are exceeded for too long, or even only crossed with rapid return to regimes within specified limits, may lead to system safety issues in addition to performance loss. Further constraints may arise due to the use of non-standard materials, designs, or both.

3.3. Degradation phenomena and failure scenarios

Failure of parts or components (in the SOFC unit) can have multiple causes. For example, failures can occur because of material discontinuities on a micro-scale which develop further over time. Stacks may also fail prematurely during operation because of collapse of one or more layers. Cracks in seals and cells can cause internal fires leading to the formation of hot spots, oxidation or excessive FU, or all of the above [21]. Failures may occur because one or several constraints are exceeded as a result of deliberately changing operation conditions or due to degradation. The nature of failures is stochastic and their prediction is thus difficult (or even impossible), especially for complex systems comprising degradation and failure susceptible system units, such as SOFCs.

Significant efforts have been made to better understand degradation mechanisms, including interface stability, redox stability, phase stability, microstructure and morphology stability, and mechanical stability (see Ref. [65] and references therein), because they affect overall performance and lifetime of the hybrid system. For commercialization of SOFCs degradation rates on a cell level of one percent have been defined as target [66]. Their time scales are usually relatively large in comparison to changes in operation setpoints. Both, degradation and failure are likely to accelerate further degradation or failure. Depending on the size of components degradation and risk of failure are not homogeneously distributed [17], in particular in complex assemblies such as fuel cells, and even less so in fuel cell stacks. Degradation mechanisms may overlap with effects in either direction, hence enhancing or compensating individual mechanisms. Aging of the SOFC materials occurs intrinsically at operating temperatures, and different phenomena may combine to alter the materials properties and microstructure, with the common effect of decreasing the electrochemical performance of the stack. For electrodes different phenomena have been identified. For instance, impurities have the tendency to aggregate at the triple phase boundary (TPB). On the cathode side new phases can generate at the interface with the electrolyte for LSM cathodes. On the anode side, nickel sintering decreases the TPB area. Degradation depends on the primary materials, manufacturing as well as assembly processes. The conductivity in commonly used YSZ electrolyte material decreases over time due to phase

Table 2

Set of controlled and manipulated variables for the SOFC system in Fig. 2.

controlled variable	manipulated variable
electrical system power (P_{AC})	electrical current (I)
mean solid temperature of SOFC stack(s) (\bar{T}_s)	blower capacity/mass flow of air (\dot{m}_{air})
FU of SOFC stack(s) (FU)	fuel valve opening/mass flow of fuel to stack(s) (\dot{m}_{fuel})
pressure gradient across solid of SOFC stack(s) & HXs (ΔP)	use of throttles (not shown in Fig. 2)
combustion outlet temperature	fuel valve opening/mass flow of fuel to combustor
air temperature to SOFC stack(s) (T_{air})	bypass ratio of air (not used here)
chemical kinetics in SOFC stack(s)	fuel composition ($X_{i,fuel}$) (not used here)

Table 3
Design and operation constraints for process units of the SOFC system in Fig. 2.

process unit	constraint	potential effect	limit
SOFC interconnect	max. leakage rate (interconnects)	performance loss, failure due to leakage	0.1% [57–60]
SOFC	power density	increasing currents lead to higher concentration polarization and faster cell degradation	80–90% of max. power density [58–60]
SOFC	max. impurities concentration	performance loss, degradation, failure	30% [58–60]
SOFC	min. temperature	performance loss, and failure due to thermo-mechanical stresses	900 K [58–60]
SOFC	max. temperature	performance loss and failure due to thermo-mechanical stresses and chemical interaction	1300 K [58–60]
SOFC	max. difference in thermal expansion coefficients	performance loss and failure due to thermo-mechanical stresses	10–17% [58–60]
SOFC	transient temperature gradients	thermo-mechanical stresses	20 K/cm [61,62]
SOFC	steady state temperature differences in axial direction of stack	thermo-mechanical stresses	150 K [58–60]
SOFC	min. FU	thermo-mechanical stresses	40% [58–60]
SOFC	max. FU	fuel starvation, efficiency loss	90% [58–60]
SOFC, pre-heaters	max. total pressure difference between fluid streams	mechanical stress	3 bar [58–60]
SOFC	safety gas (inert gas and hydrogen)	performance loss, degradation, failure	depending on start-up/shutdown strategy [63]
combustor	air-to-fuel equivalence ratio (λ)	performance loss and emission of combustable species due to incomplete combustion	> 1
combustor	residence time	flame instability due to lean operating conditions and high thermal intensity [64]	design
combustor	(transient) fuel supply	excessive temperatures [18]	design

transformation and micro-structural changes [67]. If the reduced cell is exposed to an oxidative atmosphere reoxidation and dimensional changes occurs. This can create cracks in the fuel cell layers and lead to failure [16]. The micro-cracks can cause gas cross-over with the effect of decreasing the OCV. The stacks show strong failure probabilities in case of fuel shortage for a limited time, even if they are not loaded. Local anode reoxidation can also occur during operation. At high FU, the partial pressure of fuel can locally be close to zero. In case of strong fuel depletion the fuel atmosphere is no longer reductive and conditions for a local reoxidation of the anode can occur.

3.3.1. Modeling and simulation

Increased overpotentials in SOFC.

The dependency on temperature and current density is based on [Fig. 1 (a) and (b) in Ref. [68]]. These two data sets show cell voltage drops for several current densities ranging from 0,25 to 1,94 A/cm² at the two temperatures of 750°C [Fig. 1 (a) in Ref. [68]] and 850°C [Fig. 1 (b) in Ref. [68]], respectively. This provides the functional structure between degradation (as voltage drop) and two important operation parameters, namely current density and temperature. We split the actual extent of degradation into ohmic and activation polarization losses for the electrolyte and electrodes materials using in-house data shown in Table 4 (based on a fixed temperature).

In practical terms, we extracted reference points from [Fig. 1 (a) and (b) in Ref. [68]] to generate a table with input and output parameter values. With the help of the regression software DataFit [69] a set of regression functions are generated to fit the data (statistical properties are reported for comparison). In addition to overall performance of the function, the form of the empirical function for degradation was carefully selected following several principles. The function should be defined for the entire range of interest with monotonic dependencies without overfitting and no singularities to avoid potential oscillations between given data points, which, in the worst case, can lead to excessive and negative model predictions and thus non-physical behavior. Furthermore, we follow the principle of parsimony with respect to the number of

parameters that need to be controlled. The empirical function for the degradation rates (ohmic and activation polarization loss) is

$$\dot{r}_{deg} = a_1 i^{a_2} a_3^{T_s}, \quad (18)$$

with parameter values shown in Table 5. In Ref. [70] FU was used as an additional parameter that directly affects the degradation rate. This parameter was not included here because FU is, among others, composed of electrical current which is already considered. Our tests showed worse performance and some loss of control in the model.

Overall, the behavior with respect to temperature and current density within the operation regime is as follows: At constant temperature the degradation rate increases with higher current density, and at constant current density the degradation rate decreases with higher temperature (unless the higher temperature limit is exceeded). The first statement is in line with the data in Ref. [68], and the second statement with the data in Ref. [71]. This approach allows us to calculate spatially distributed degradation rates in the SOFC module.

3.3.1.1. Fouling and erosion in preheaters. Preheaters are assumed to be made of ceramic materials that can withstand elevated temperatures. Metals have better manufacturability, weldability as well as mechanical properties, such as strength and ductility. They have an upper temperature limit [72], but this limit is higher than that critical for our application. Ceramics have relatively high temperature limits and low susceptibility to fouling [73], this degradation mechanism is therefore neglected. But mechanical strength may be an issue [73] and thus shock resistance, for example during system start-up.

3.3.1.2. Degradation in combustor. Unless novel technology is used for the combustor, for example in terms of materials, operation conditions [57] or feedstocks, it is probably not the direct cause for performance deterioration of the system. Degradation could potentially lead to changes in outlet temperature profiles, but high combustion efficiencies may be maintained [74].

Table 4
Degradation rates for ohmic and activation polarization losses in SOFC.

part	degradation phenomenon	degradation rate [1/1.000 h]	degradation cause	effects of degradation
electrolyte	increased ohmic losses	0,007–0008	micro-domain formation & grain-boundary segregation	reduction in ohmic conductivity
cathode	increased ohmic losses	< 0,001	micro-structural changes under operation conditions	increase in area-specific ohmic resistance
anode	increased ohmic losses	0,01–0,013	micro-structural changes	increase in area-specific ohmic resistance
cathode	increased activation polarization losses	0,004–0006	micro-structural changes	increase in cathode overpotential
anode	increased activation polarization losses	0,02–0,03	micro-structural changes	increase in anode overpotential

Table 5
Parameters (approximated) of regression function for degradation rate in Equation (18).

parameter	$\dot{r}_{deg,ohm}$	$\dot{r}_{deg,act}^{an}$	$\dot{r}_{deg,act}^{ca}$
a_1	38,17	56,62	10,91
a_2	0,99	0,99	0,99
a_3	3,1	3,1	3,1

3.3.1.3. Failure scenarios. The failure scenario analysed here is the breakage of interconnects which causes loss of one SOFC stack. The failure is initiated after 100 s. Interconnects connect the anode of one cell with the cathode of the adjacent cell, preventing mixing of fuel and air (or oxygen-rich gas). Despite a stronger emphasis in the technical literature on the electrochemical cell, interconnects play a key role in the technological realization of SOFC-based systems. The main physical requirements for interconnects are high electronic conductivity, chemical stability in reducing and oxidizing atmospheres on the anode and cathode side, respectively at operation temperatures, gas tightness and matching thermal expansion coefficient of connecting materials [36,75]. In the assumed failure scenario, hydrogen on the anode side would mix with air from the cathode side inevitably leading to ignition or explosion. Unless the stacks that are subject to such failures are immediately isolated, an emergency shutdown is likely to be required with a sudden loss in power and possibly irreversibly damage of all stacks and cells in the SOFC unit.

To meet safety requirements and to maintain power generation during aforementioned failure scenarios, cells are modularized. Here, $M = 48$ cells are bundled into $N = 25$ stacks, Fig. 3 provides some details. The total number of cells was based on the design in Ref. [9], and the split in N stacks and M cells was based on technological and economic feasibility, but other combinations are also possible. It is assumed that power demand remains constant. Setpoints of manipulated variables are obtained by operation of all stacks. These remain constant while fewer stacks are available for the same power demand. Traditional controllers (for power generation applications) are usually developed and tuned for the range of interest for all variables, without taking into account drifts of setpoints due to degradation and failure (or only to some extent). With the use of advanced control strategies, such as nonlinear model predictive control (NMPC) [76,77], new setpoints of manipulated variables are automatically defined by the optimization algorithm to keep controlled variables constant. NMPC applications are not further discussed here, but probably add benefits in terms of performance as well as lifetime of SOFC systems components.

3.4. Model implementation

The process system model is implemented in gPROMS which is essentially an advanced equation solver for complex dynamic large-scale problems. The solvers require a well-posed problem formulation. In other words, an equal number of unknown and equations, which is utilized in the degrees of freedom analysis discussed above. The model must be formulated as an index one problem. Definition of upper and lower bounds on each variable improve numerical stability and act as check for physical behavior. The system model consists of more than 5500 algebraic and more than 1300 differential equations. A number of 40 discretization elements in axial direction in the SOFC model is used to balance accuracy and computational calculation cost. We employ finite difference schemes for the discretization of the PDE, i.e. central, forward or backward differences for gases and solid phases, respectively. Differential-algebraic equations are numerically solved using the DAEBDF solver. For all simulations steady state is defined as initial condition. The actual physical models representing process units are extended by cross-check functions on all hierarchy levels to ensure physical behavior. For linear algebraic equations, the MA48 solver is used, which is based on a direct LU-factorization algorithm (see Ref. [78] for further information). For nonlinear equations the BDNLSOL solver is used. Both, the DASOLV and SRADAU solvers were tested, which showed comparable or worse performance than the DAEBDF solver. Physical properties are called from the physical property package Multiflash or taken from literature. A Soave-Redlich-Kwong equation of state is used with volume shift of Peneloux volume shift and van der Waals mixing rules [79].

4. Results and discussion

In the first part of this section results from steady-state simulations at the design point are presented. In the second part, we discuss results of transient system responses to failure at constant power output. In the third part, simulation results for degradation are presented.

For model verification we calculate the overall steady state deviation of energy and mass conservation between inlet and outlets of system components based on

$$\Delta\zeta = 1 - \frac{\sum_k \zeta_{in,k}}{\sum_k \zeta_{out,k}}, \quad \zeta = \dot{E}, \dot{m}. \quad (19)$$

Deviations occur due to numerics, for the SOFC unit for example which is the most complex system component, the deviation with respect to energy is about 0,1% and for mass about 0,001%. This accuracy is considered as sufficient for a system analysis.

4.1. System performance in design point

Fig. 2 shows key inputs and simulation results. In the design point the FU is 0,75, the mean solid temperature is 1260 K and the AC power output set to 170 kW. The resulting overall system efficiency is about 31% which is within the range reported in Ref. [80]. As mentioned earlier, higher system efficiencies can be achieved with waste heat recovery methods and other fuels. Using hydrogen as fuel however has advantages for applications where emissions are of concern. Besides, carbon-containing fuels require additional process equipment, for example for pre-reforming of natural gas or other gaseous hydrocarbons. In addition to higher system complexity further constraints need then to be considered. Moreover, following a design process in which efficiency is maximized, for example by using additional heat exchangers, may lead to difficulties during start-up and could also add further potential failure modes. Due to the assumed non-ideal DC/AC converter, 9,5 kW of power are dissipated. In the combustor all remaining combustible species (here hydrogen) are consumed, which increases the heat content in the gas utilized for pre-heating. The system has a relatively high degree of thermal coupling, and therefore a strong effect on the operating envelope and constraints.

4.2. Effect of failure of an SOFC stack on system performance

The SOFC unit originally consists of $N = 25$ stacks with $M = 48$ cells each. The simulated failure scenario is the loss of one stack as shown in Fig. 5, which is initiated after 100 s. The total power output (external load requirements) are kept constant. Operation at constant power output, i.e. the absence of thermal or redox cycles, represents a rather benign operation method for the system. In contrast, transient operation with changing power demand can lead to extensive drifts in physical quantities and can therefore be critical for the system. Fig. 6 shows the system's response in terms of cell voltage and current. The stacks in operation need to compensate the power requirement of the failed stack, which leads to a rapid increase in cell current while the cell voltage drops. A new steady state is reached after about 300 s. The maximum total current density is 0,64 A/cm² before it reached the new steady state of 0,57 A/cm². Rapid transients in current density can have a detrimental effect on the lifetime of the SOFC stacks. Fig. 7 shows the FU which increased from 0,75 to 0,8 with a maximum of 0,88. An FU of 0,85 for example could lead to fuel starvation during such a failure incident. Fig. 8 shows the solid temperature of the SOFC stacks over the axial direction at initial time ($t = 0$) and after 1600 s. In some parts the temperature increased beyond the limit (see Table 3). The design operation envelope should therefore include constraints with potentially additional contingency, depending on the general operation strategy, i.e. frequently imposed transients or operation mostly in steady state. An overall conclusion is that the SOFC unit responded relatively quickly to this type of failure, i.e. where power density

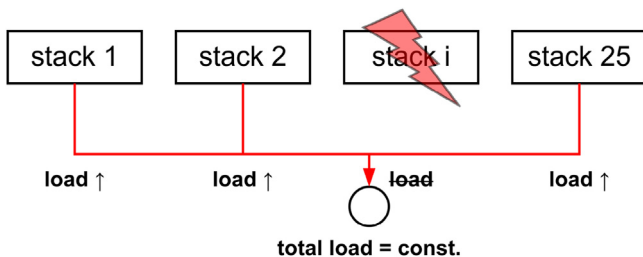


Fig. 5. Simulated failure mode - loss of one stack.

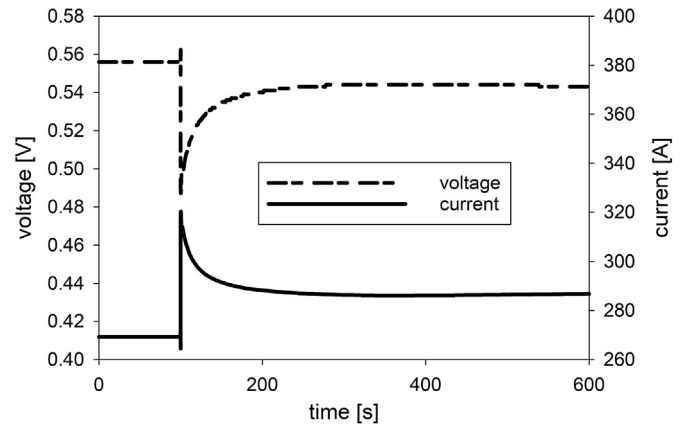


Fig. 6. Cell current and voltage in SOFC stacks over time for the case of failure of one stack.

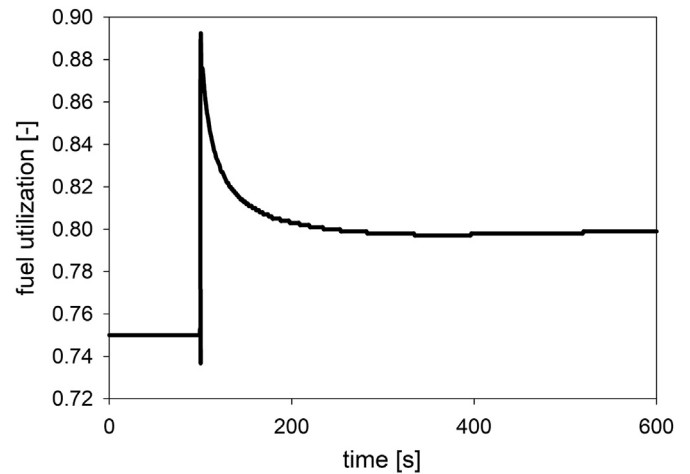


Fig. 7. Fuel utilization in SOFC stacks over time for the case of failure of one stack.

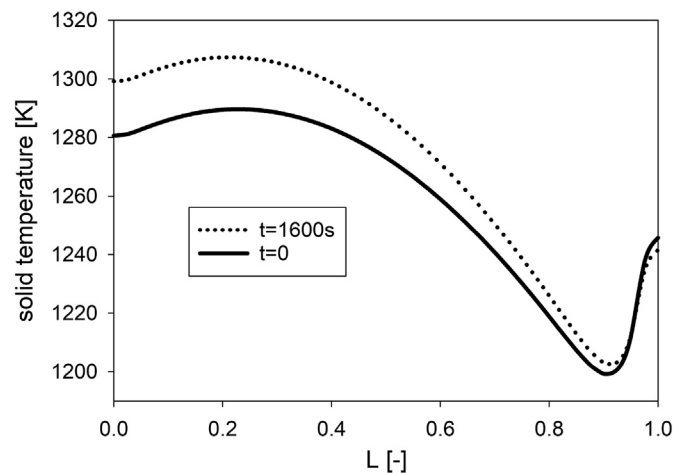


Fig. 8. Solid temperature in SOFC stacks at $t = 0$ and $t = 1600$ s for the case of failure of one stack.

per stack in the SOFC unit increases. The balance-of-plant system components add inertia which smooth transients. Effects of degradation are in this failure case negligible because of the

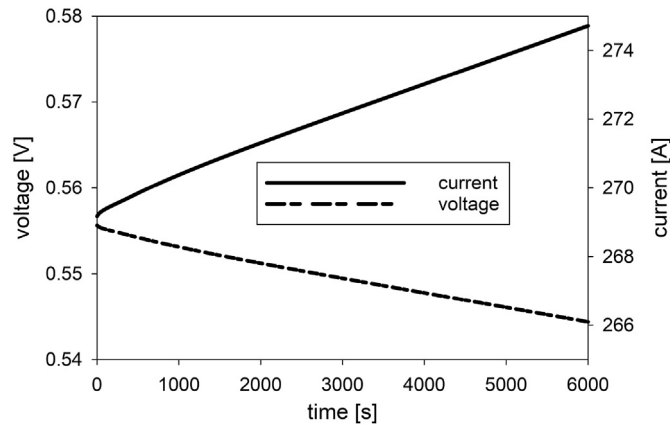


Fig. 9. Current and voltage in SOFC stacks over time for the case of degradation.

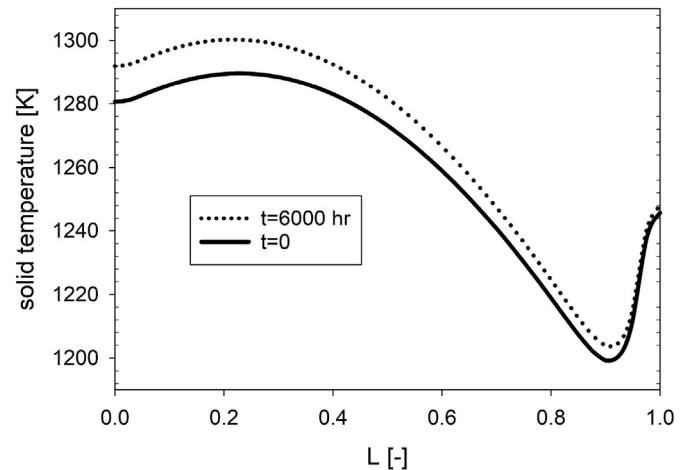


Fig. 10. Solid temperature in SOFC stacks at $t = 0$ and $t = 6000$ h for the case of degradation.

relatively short time period.

4.3. Effect of degradation in the SOFC on system performance

Degradation usually occurs in longer time periods compared to deliberate changes in operation conditions such as part-load operation. Whereas operation of the system is within minutes time constants of degradation are usually in the order of several hundred hours. However, substantial degradation with potential failure can also occur in much shorter time frames. A case in point is during start-up and shutdown or generally cycling, operation under critical conditions, and as response to external disturbances (e.g., impurities in the supplied fluids). Fig. 9 shows the cell current and voltage over a time period of 6000 h. Degradation leads to higher overpotential losses and hence reduce cell voltages. The current increased from 269 A to 275 A. The voltage SOFC is frequently used as degradation signal to report its extent [81] while current density constant is kept constant [68]. From a power consumer-perspective however, the delivery of a constant power is usually required and therefore assumed here. The degradation rate varies with current density and temperature, but overall values calculated here are within single digit percentages per 1000 h, similar to those reported in Refs. [82–84].

Fig. 10 shows the solid temperature at initial time ($t = 0$) and after 6000 h. The solid temperature of some parts of the SOFC stack exceeded the limit (see Table 3). Operation conditions should be corrected by the controllers after operation of the system for several thousand hours to compensate for the drift in critical parameters, such as the solid temperature. The cumulative effect of degradation, critical operation conditions and the failure type discussed above could bring the SOFC unit in a critical operation regime where failure probability increases, potentially in an accelerated fashion.

4.4. Practical implications

The physical phenomena in SOFC systems are complex and take place in a relatively wide range in the time and spatial domain, as discussed above. By restriction on individual though critical parts of the SOFC system, other potential failure modes, possibly introduced by balance-of-plant components, may be missed. Collection of design and operational constraints for all system components is hence of practical importance and is emphasized in this work.

Furthermore, design and optimization for one (or few) thermodynamic, economic, or environmental specification⁵ may compromise reliability, flexibility and other metrics of the system. Instead, a balanced design process should be applied that takes into account constraints and a certain contingency to compensate for transient performance deterioration phenomena. It is shown that failure of one out of 25 stacks in the SOFC unit already has a relatively strong detrimental effect on performance with a shift of operation conditions towards higher criticality. A more advanced control strategy may be required for a proper pairing of controlled and manipulated variables because of mutual interactions [56]. The identification of controlled and manipulated variables is also emphasized in this work, because it allows to estimate the system's transient flexibility more realistically as (irreversible) degradation accumulates over time. In summary, constraints and degree of freedom analyses should go hand in hand with the design and selection of materials for technically and economically feasible operation of the SOFC-based system, as summarized in Fig. 1.

4.5. Uncertainties and limitations of this study

One limitation of this work is, as generally for analyses on a system-level, that probably not all potential (mutually affecting) influences are taken into account for degradation and failure phenomena. This is presumably inevitable because manufacturing and assembly for example also have an effect on how degradation and failure will evolve in actual parts.

Data availability is another limitation, which is often the case in system modeling studies. In particular spatially distributed quantities during transients are experimentally difficult to obtain, if at all. But collaboration between theorists and experimentalists can support the identification of physical quantities which, on one hand, are experimentally obtainable, and on the other hand, pivotal for the physical phenomena to be modeled. More specifically, the empirical function used for modeling ohmic and activation polarization losses has a limited range with respect to its parameter-dependency. Degradation rates are probably much higher during start-up and shutdown with an associated strong effect on failure probability. This may be the case even though these transients last only a couple of hours. Furthermore, potential shocks in unpurged fluid channels or electrical connections can be promoted. As a result, the system may be in a different state with respect to degree of degradation once it is brought to operation.

⁵ See Ref. [85] for a review.

5. Conclusions

In this work, degradation and failure on a system level was investigated. A parameter-dependent and spatially distributed degradation rate function for ohmic and activation polarization losses in the SOFC stacks is developed. Irreversible loss in cell voltage is dependent on the operation history of the system, rather than on the effective age of system components. Degradation and failure of whole stacks lead to drifts and shifts in physical quantities, such as temperature and current density. This needs to be considered when developing and tuning controllers to maintain proper operation. Failure of parts probably has an immediate effect on the overall system performance, but this depends on the type and extent of the failure. It should be noticed that there are generally few studies investigating failure on a fuel cell system level using a detailed physics-based approach [86,87], rather than one based on statistical models [81,88,89].

Dynamic system responses in electrical quantities were assumed to occur instantaneously. The use of overall degradation rates that are frequently reported in the technical literature may be misleading, because the rate of degradation can vary significantly for different sections of the SOFCs. Some parts may show (almost) negligible degradation whilst others may be severely degraded. In the latter case the risk of failure is more likely. A better understanding of parameter- and history dependency of degradation and failure mechanisms is needed, including the identification of the physical parameters that control these mechanisms the most. A case in point is the mean solid temperature in the stack which should probably be kept constant during transient operation to stay within the safe operation envelope. This strong interlink between process design, material science, and control is an aspect to which we aim to contribute.

Apart from the specific quantitative results, perhaps the main practical contribution of this work are the collected design and operation constraints as well as the degrees of freedom analysis which results in the identification of controlled and manipulated variables. These analyses should be understood as a general procedure for analyses of systems of this type, in which knowledge from process design, material science and control engineering is combined.

Stronger collaboration between theorists and experimentalists on a system level would probably lead to accelerated advancements in the research and development of SOFC systems. For example, experimentalists can provide figures for measurable quantities, which can then be used by theorists to model physical phenomena, calibrate models, or both.

Potential extensions of this work include: (i) replacing the degradation rate function with a probability distribution of the physical variables, (ii) extending the operation range of the system to cover start-up and shutdown with corresponding degradation rates and failure probabilities, (iii) extending the range of fuels including carbon-containing fuels, which would require reforming and also add further constraints as well as lead to accelerated degradation, (iv) extending the model to conduct thermo-mechanical stress analyses, (v) testing of statistical and probabilistic models (including parametric mixture distributions) which are developed by the system reliability community.

Declaration of competing interest

The authors declare that they have no known competing financial interests or personal relationships that could have appeared to influence the work reported in this paper.

Acknowledgement

Dr Christoph Stiller is gratefully acknowledged for providing the original SOFC model code. The experimental data used in this work to determine the input parameters were partly collected in framework of the project 17-79-30071 funded by the Russian Science Foundation. We thank the editors and anonymous reviewers who made it possible to substantially improve this paper.

References

- [1] van Biert L, Visser K, Aravind P. A comparison of steam reforming concepts in solid oxide fuel cell systems. *Appl Energy* 2020;264:114748.
- [2] Wang X, Lv X, Weng Y. Performance analysis of a biogas-fueled sofc/gt hybrid system integrated with anode-combustor exhaust gas recirculation loops. *Energy* 2020;197:117213.
- [3] long Wu X, wu Xu Y, qi Zhao D, bo Zhong X, Li D, Jiang J, Deng Z, Fu X, Li X. Extended-range electric vehicle-oriented thermoelectric surge control of a solid oxide fuel cell system. *Appl Energy* 2020;263:114628.
- [4] Arsalis A. A comprehensive review of fuel cell-based micro-combined-heat-and-power systems. *Renew Sustain Energy Rev* 2019;105:391–414.
- [5] Hawkes A, Leach M. Cost-effective operating strategy for residential micro-combined heat and power. *Energy* 2007;32(5):711–23.
- [6] Liso V, Olesen A, Nielsen M, Kar S. Performance comparison between partial oxidation and methane steam reforming processes for solid oxide fuel cell (sofc) micro combined heat and power (chp) system. *Energy* 2011;36(7):4216–26.
- [7] Zhang H, Xu H, Chen B, Dong F, Ni M. Two-stage thermoelectric generators for waste heat recovery from solid oxide fuel cells. *Energy* 2017;132:280–8.
- [8] Kandepu R, Imsland L, Foss B, Stiller C, Thorud B, Bolland O. Modeling and control of a sofc-gt-based autonomous power system. *Energy* 2007;32(4):406–17.
- [9] Stiller C, Thorud B, Bolland O, Kandepu R, Imsland L. Control strategy for a solid oxide fuel cell and gas turbine hybrid system. *J Power Sources* 2006;158(1):303–15.
- [10] Faro ML, Zignani S, Trocino S, Antonucci V, Aricĕw A. New insights on the co-electrolysis of co₂ and h₂o through a solid oxide electrolyzer operating at intermediate temperatures. *Electrochim Acta* 2019;296:458–64.
- [11] Frank M, Deja R, Peters R, Blum L, Stolten D. Bypassing renewable variability with a reversible solid oxide cell plant. *Appl Energy* 2018;217:101–12.
- [12] Kupecki J, Motylinski K, Jagielski S, Wierzbicki M, Brouwer J, Naumovich Y, Skrzypliewicz M. Energy analysis of a 10 kw-class power-to-gas system based on a solid oxide electrolyzer (soe)199. " *Energy Conversion and Management*; 2019.
- [13] Hubert M, Laurencin J, Cloetens P, Morel B, Montinaro D, Lefebvre-Joud F. Impact of nickel agglomeration on solid oxide cell operated in fuel cell and electrolysis modes. *J Power Sources* 2018;397:240–51.
- [14] Laurencin J, Hubert M, Sanchez DF, Pylypko S, Morales M, Morata A, Morel B, Montinaro D, Lefebvre-Joud F, Siebert E. Degradation mechanism of la_{0.6}sr_{0.4}co_{0.2}fe_{0.8}o_{3-d}/gd_{0.1}ce_{0.9}o_{2-d} composite electrode operated under solid oxide electrolysis and fuel cell conditions. *Electrochim Acta* 2017;241:459–76.
- [15] Minh NQ, Mogensen MB. Reversible solid oxide fuel cell technology for green fuel and power production. *The Electrochemical Society Interface* 2013;22(4).
- [16] Bujalski W, Dikwal C, Kendall K. Cycling of three solid oxide fuel cell types. *J Power Sources* 2007;171(1):96–100. *Scientific Advances in Fuel Cell Systems*, Turin, Italy, 13–14 September 2006.
- [17] Chatzichristodoulou C, Chen M, Hendriksen P, Jacobsen T, Mogensen M. Understanding degradation of solid oxide electrolysis cells through modeling of electrochemical potential profiles. *Electrochim Acta* 2016;189:265–82.
- [18] Mueller F, Jabbari F, Brouwer J. On the intrinsic transient capability and limitations of solid oxide fuel cell systems. *J Power Sources* 2009;187(2):452–60.
- [19] Bessler W, Gewies S, Vogler M. A new framework for physically based modeling of solid oxide fuel cells. *Electrochim Acta* 2007;53(4):1782–800.
- [20] Zhu H, Kee R. A general mathematical model for analyzing the performance of fuel-cell membrane-electrode assemblies. *J Power Sources* 2003;117(1–2):61–74.
- [21] Ahmed K, Foger K. Perspectives in solid oxide fuel cell-based microcombined heat and power system. *ASME. J. Electrochem. En. Conv. Stor.* 2017;14(3). 031005 (12 pages).
- [22] Yokokawa H, Tu H, Iwanschitz B, Mai A. Fundamental mechanisms limiting solid oxide fuel cell durability. *J Power Sources* 2008;182(2):400–12.
- [23] Yan D, Liang L, Yang J, Zhang T, Pu J, Chi B, Li J. Performance degradation and analysis of 10-cell anode-supported sofc stack with external manifold structure. *Energy* 2017;125:663–70.
- [24] Ma Z, Jiang J, Shi W, Zhang W, Mi C. Investigation of path dependence in commercial lithium-ion cells for pure electric bus applications: aging mechanism identification. *J Power Sources* 2015;274:29–40.
- [25] Bird RB, Stewart WE, Lightfoot EN. *Transport phenomena*. Wiley; 2006.
- [26] DeCaluwe SC, Weddle PJ, Zhu H, Colclasure AM, Bessler WG, Jackson GS, Kee RJ. On the fundamental and practical aspects of modeling complex

- electrochemical kinetics and transport. *J Electrochem Soc* 2018;165(13):E637–58.
- [27] Dicks AL, Rand DAJ. Fuel cell systems explained. John Wiley & Sons Ltd.; 2018.
- [28] Gellings PJ, Bouwmeester HJ. Handbook of solid state electrochemistry. CRC; 1997.
- [29] Kee RJ, Coltrin ME, Glarborg P, Zhu H. Chemically reacting flow: theory, modeling, and simulation. Wiley; 2018.
- [30] O'Hayre R, Cha S, Colella W, Prinz F. Fuel cell fundamentals. John Wiley & Sons.; 2009.
- [31] Cai R, Gou C. A proposed scheme for coal fired combined cycle and its concise performance. *Appl Therm Eng* 2007;27(8–9):1338–44.
- [32] Peters R, Deja R, Blum L, Pennanen J, Kiviahio J, Hakala T. Analysis of solid oxide fuel cell system concepts with anode recycling. *Int J Hydrogen Energy* 2013;38(16):6809–20.
- [33] Kee R, Zhu H, Goodwin D. Solid-oxide fuel cells with hydrocarbon fuels, 30 II; 2005. p. 2379–404.
- [34] Lanzini A, Ferrero D, Papurello D, Santarelli M. Reporting degradation from different fuel contaminants in ni-anode sofc. *Fuel Cell* 2017;17(4):423–33.
- [35] Nakajo A, Wuillemin Z, Metzger P, Diethelm S, Schiller G, Van Herle J, Favrat D. Electrochemical model of solid oxide fuel cell for simulation at the stack scale i. calibration procedure on experimental data. *J Electrochem Soc* 2011;158(9):B1083–101.
- [36] Aicart J, Kuhn J, Kesler O. Performance of non-destructive compressive seals for reversible solid oxide cells. *Fuel Cell* 2017;17(1):90–9.
- [37] Fergus JW. Solid oxide fuel cells. John Wiley & Sons, Ltd; 2012. p. 671–700. ch. 14.
- [38] Huang K, Singhal S. Cathode-supported tubular solid oxide fuel cell technology: a critical review. *J Power Sources* 2013;237:84–97.
- [39] Li P-W, Chyu MK. Simulation of the chemical/electrochemical reactions and heat/mass transfer for a tubular sofc in a stack. *J Power Sources* 2003;124(2):487–98.
- [40] Cooper SJ, Brandon NP. Chapter 1 - an introduction to solid oxide fuel cell materials, technology and applications. In: Brandon NP, Ruiz-Trejo E, Boldrin P, editors. *In solid oxide fuel cell Lifetime and reliability*. Academic Press; 2017. p. 1–18.
- [41] Jamil SM, Othman MHD, Rahman MA, Jaafar J, Ismail A, Li K. Recent fabrication techniques for micro-tubular solid oxide fuel cell support: a review. *J Eur Ceram Soc* 2015;35(1):1–22.
- [42] Li T, Heenan T, Rabuni M, Wang B, Farandos N, Kelsall G, Matras D, Tan C, Lu X, Jacques S, Brett D, Shearing P, Di Michiel M, Beale A, Vamvakeros A, Li K. Design of next-generation ceramic fuel cells and real-time characterization with synchrotron x-ray diffraction computed tomography. *Nat Commun* 2019;10(1).
- [43] Stiller C. Design, operation and control modelling of SOFC/GT hybrid systems. PhD thesis. NTNU; 2006.
- [44] Doraswami U, Droushiotis N, Kelsall G. Modelling effects of current distributions on performance of micro-tubular hollow fibre solid oxide fuel cells. *Electrochim Acta* 2010;55(11):3766–78.
- [45] Bao C, Wang Y, Feng D, Jiang Z, Zhang X. Macroscopic modeling of solid oxide fuel cell (sofc) and model-based control of sofc and gas turbine hybrid system. *Prog Energy Combust Sci* 2018;66:83–140.
- [46] Bove R, Lunghi P, Sammes NM. Sofc mathematic model for systems simulations. part one: from a micro-detailed to macro-black-box model. *Int J Hydrogen Energy* 2005;30(2):181–7. Fuel Cells.
- [47] Hajimolana SA, Hussain MA, Daud WAW, Soroush M, Shamiri A. Mathematical modeling of solid oxide fuel cells: a review. *Renew Sustain Energy Rev* 2011;15(4):1893–917.
- [48] Kakac S, Pramuanjaroenkij A, Zhou XY. A review of numerical modeling of solid oxide fuel cells. *Int J Hydrogen Energy* 2007;32(7):761–86. Fuel Cells.
- [49] Amiri S, Hayes R, Sarkar P. Transient simulation of a tubular micro-solid oxide fuel cell. *J Power Sources* 2018;407:63–9.
- [50] Bianchi F, Bosio B, Baldinelli A, Barelli L. Optimization of a reference kinetic model for solid oxide fuel cells. *Catalysts* 2020;10(1).
- [51] Min G, Park YJ, Hong J. 1d thermodynamic modeling for a solid oxide fuel cell stack and parametric study for its optimal operating conditions. *Energy Convers Manag* 2020;209:112614.
- [52] Noren D, Hoffman M. Clarifying the butler-volmer equation and related approximations for calculating activation losses in solid oxide fuel cell models. *J Power Sources* 2005;152(1–2):175–81.
- [53] Smith J, Ness HV, Abbott M. Introduction to chemical engineering thermodynamics. Wiley; 2005.
- [54] Halinen M, Thomann O, Kiviahio J. Experimental study of sofc system heat-up without safety gases. *Int J Hydrogen Energy* 2014;39(1):552–61.
- [55] Cengel Y. Heat and mass transfer. McGraw Hill; 2007.
- [56] Skogestad S, Postlethwaite I. Multivariable feedback control: analysis and design. Wiley; 2005.
- [57] Colombo K, Bolland O, Khartou V, Stiller C. Simulation of an oxygen membrane-based combined cycle power plant: Part-load operation with operational and material constraints. *Energy Environ Sci* 2009;2(12):1310–24.
- [58] Vielstich W, Lamm A, Gasteiger HA, editors. Handbook of fuel cells, vol. 5. Wiley; 2009.
- [59] Vielstich W, Lamm A, Gasteiger HA, editors. Handbook of fuel cells, vol. 6. Wiley; 2009.
- [60] NETL. Fuel cell handbook. US Department of Energy; 2004.
- [61] Kim-Lohsoontorn P, Priyakorn F, Wetwatana U, Laosiripojana N. Modelling of a tubular solid oxide fuel cell with different designs of indirect internal reformer. *Journal of Energy Chemistry* 2014;23(2):251–63.
- [62] Spivey B, Edgar T. Dynamic modeling, simulation, and mimo predictive control of a tubular solid oxide fuel cell. *J Process Contr* 2012;22(8):1502–20. Ken Muske Special Issue.
- [63] Engelbracht M, Peters R, Tiedemann W, Hoven I, Blum L, Stolten D. An on-demand safety gas generator for solid oxide fuel cell and electrolyzer systems. *Fuel Cell* 2017;17(6):882–9.
- [64] Shantanu M, Reddy VM, Karmakar S. Experimental and numerical studies on heat recirculated high intensity meso-scale combustor for mini gas turbine applications. *Energy Convers Manag* 2018;176:324–33.
- [65] Jin X, Xue X. Modeling of chemical-mechanical couplings in anode-supported solid oxide fuel cells and reliability analysis. *RSC Adv* 2014;4(30):15782–96.
- [66] Zhu J, Lin Z. Degradations of the electrochemical performance of solid oxide fuel cell induced by material microstructure evolutions. *Appl Energy* 2018;231:22–8.
- [67] Larrain D, herle JV, Favrat D. Simulation of sofc stack and repeat elements including interconnect degradation and anode reoxidation risk. *J Power Sources* 2006;161(1):392–403.
- [68] Hagen A, Barfod R, Hendriksen P, Liu Y-L, Ramousse S. Degradation of anode supported sofc as a function of temperature and current load. *J Electrochem Soc* 2006;153(6):A1165–71.
- [69] Oakdale engineering develops datafit. 2006.
- [70] Cuneo A, Zaccaria V, Tucker D, Traverso A. Probabilistic analysis of a fuel cell degradation model for solid oxide fuel cell and gas turbine hybrid systems. *Energy* 2017;141:2277–87.
- [71] Primdahl S, Mogensen M. Durability and thermal cycling of ni/ysz cermet anodes for solid oxide fuel cells. *J Appl Electrochem* 2000;30(2):247–57.
- [72] Zhang X, Keramati H, Arie M, Singer F, Tiwari R, Shooshitari A, Ohadi M. Recent developments in high temperature heat exchangers: a review. *Frontiers in Heat and Mass Transfer* 2018;11.
- [73] Sommers A, Wang Q, Han X, T'Joen C, Park Y, Jacobi A. Ceramics and ceramic matrix composites for heat exchangers in advanced thermal systems-a review. *Appl Therm Eng* 2010;30(11–12):1277–91.
- [74] Kurz R BK. Degradation in gas turbine systems. *J Eng Gas Turbines Power* 2001;123(1):70–7.
- [75] Vielstich W, Lamm A, Gasteiger HA, editors. Handbook of fuel cells, vol. 4. Wiley; 2003.
- [76] Diehl M, Bock H, Schloder J, Findeisen R, Nagy Z, Allgower F. Real-time optimization and nonlinear model predictive control of processes governed by differential-algebraic equations. *J Process Contr* 2002;12(4):577–85.
- [77] Henson MA. Nonlinear model predictive control: current status and future directions. *Comput Chem Eng* 1998;22(2):187–202.
- [78] Golub G, Loan CV. Matrix computations. Johns Hopkins University Press; 2013.
- [79] Process systems enterprise. the advanced process modelling company.™.
- [80] Staffell I, Scamman D, Velazquez Abad A, Balcombe P, Dods P, Ekins P, Shah N, Ward K. The role of hydrogen and fuel cells in the global energy system. *Energy Environ Sci* 2019;12(2):463–91.
- [81] Wu X, Ye Q. Fault diagnosis and prognostic of solid oxide fuel cells. *J Power Sources* 2016;321:47–56.
- [82] Hornes A, Torrell M, Morata A, Kendall M, Kendall K, Tarancón A. Towards a high fuel utilization and low degradation of micro-tubular solid oxide fuel cells. *Int J Hydrogen Energy* 2017;42(19):13889–901. Special Issue on The 21st World Hydrogen Energy Conference (WHEC 2016), 13–16 June 2016, Zaragoza, Spain.
- [83] Minh N. Solid oxide fuel cells for power generation and hydrogen production. *Journal of the Korean Ceramic Society* 2010;47(1):1–7.
- [84] Stoeckl B, Preininger M, Subotic V, Megel S, Folgner C, Hochenauer C. Towards a wastewater energy recovery system: the utilization of humidified ammonia by a solid oxide fuel cell stack. *J Power Sources* 2020;450:227608.
- [85] Ramadhani F, Hussain M, Mokhlis H, Hajimolana S. Optimization strategies for solid oxide fuel cell (sofc) application: a literature survey. *Renew Sustain Energy Rev* 2017;76:460–84.
- [86] Kupecki J, Motylinski K, Zurawska A, Kosiorek M, Ajdys L. Numerical analysis of an sofc stack under loss of oxidant related fault conditions using a dynamic non-adiabatic model. *Int J Hydrogen Energy* 2019;44(38):21148–61. Special Issue on HYPOTHESIS XIII.
- [87] Xiao-Long W, Yuan-Wu X, Tao X, Xi L. Fault modeling and simulation of pure hydrogen solid oxide fuel cell system. 2017. p. 2688–92. 2017-January.
- [88] Astrom K, Fontell E, Virtanen S. Reliability analysis and initial requirements for fc systems and stacks. *J Power Sources* 2007;171(1):46–54. Scientific Advances in Fuel Cell Systems, Turin, Italy, 13–14 September 2006.
- [89] Costamagna P, Giorgi AD, Moser G, Pellaco L, Trucco A. Data-driven fault diagnosis in sofc-based power plants under off-design operating conditions. *Int J Hydrogen Energy* 2019;44(54):29002–6.